

## A suitable model for emeraldine salt

Adrián Varela-Álvarez and José A. Sordo

Citation: *J. Chem. Phys.* **128**, 174706 (2008); doi: 10.1063/1.2913246

View online: <http://dx.doi.org/10.1063/1.2913246>

View Table of Contents: <http://jcp.aip.org/resource/1/JCPSA6/v128/i17>

Published by the [American Institute of Physics](#).

---

### Related Articles

Statics of polymer droplets on deformable surfaces

*J. Chem. Phys.* **135**, 214703 (2011)

Interactions between polymer brush-coated spherical nanoparticles: The good solvent case

*J. Chem. Phys.* **135**, 214902 (2011)

Solvent response of mixed polymer brushes

*J. Chem. Phys.* **135**, 214901 (2011)

Polymer solar cells with gold nanoclusters decorated multi-layer graphene as transparent electrode

*APL: Org. Electron. Photonics* **4**, 259 (2011)

Polymer solar cells with gold nanoclusters decorated multi-layer graphene as transparent electrode

*Appl. Phys. Lett.* **99**, 223302 (2011)

---

### Additional information on *J. Chem. Phys.*

Journal Homepage: <http://jcp.aip.org/>

Journal Information: [http://jcp.aip.org/about/about\\_the\\_journal](http://jcp.aip.org/about/about_the_journal)

Top downloads: [http://jcp.aip.org/features/most\\_downloaded](http://jcp.aip.org/features/most_downloaded)

Information for Authors: <http://jcp.aip.org/authors>

### ADVERTISEMENT

**AIP**Advances

*Submit Now*

**Explore AIP's new  
open-access journal**

- **Article-level metrics  
now available**
- **Join the conversation!  
Rate & comment on articles**

## A suitable model for emeraldine salt

Adrián Varela-Álvarez and José A. Sordo<sup>a)</sup>

Laboratorio de Química Computacional, Departamento de Química Física y Analítica,  
Facultad de Química, Universidad de Oviedo, C/ Julián Clavería 8, 33006 Oviedo,  
Principado de Asturias, Spain

(Received 15 January 2008; accepted 27 March 2008; published online 6 May 2008)

A new mechanism for the formation of doped polyaniline is presented. Besides providing suitable structural and spectroscopic parameters, the new mechanism allows for the rationalization of the experimentally observed equilibrium between polaron and bipolaron defects in emeraldine salt. The magnetic behavior and the “metallic island” model for conduction in doped polyaniline are also theoretically supported by the new proposal. © 2008 American Institute of Physics.

[DOI: [10.1063/1.2913246](https://doi.org/10.1063/1.2913246)]

### INTRODUCTION

In 2000, MacDiarmid, Heeger, and Shirakawa were awarded a Nobel Prize for the discovery and development of conductive polymers.<sup>1,2</sup> As MacDiarmid emphasized in a recent article,<sup>3</sup> it is a multidisciplinary field of great interest for chemists, electrochemists, biochemists, experimental and theoretical physicists, and electronic and electrical engineers due to the important technological emerging applications of these materials.

In a seminal article,<sup>4</sup> Stafström *et al.* proposed a mechanism to explain the huge increase (about ten orders of magnitude) in electrical conductivity when doping polyaniline (PANI) with HCl. According to such a mechanism, protonation of semiconductor emeraldine base (EB) leads to a spinless structure (bipolaron), which rearranges to a charged radical open-shell structure (two polarons) that finally splits into two polaron units [emeraldine salt (ES)]. However, Heeger recently complained that “*there is no calculations showing that the metallic (emeraldine salt) final state is lower in energy than the semiconductor and there is no detailed understanding of the rearrangement reactions*” [in the proposed mechanism].<sup>5</sup>

Although recent theoretical works<sup>6–8</sup> have greatly contributed to the understanding of the experimental behavior exhibited by doped PANI, a number of fundamental questions remain to be uncovered, namely, (a) the mechanism proposed by Stafström *et al.*<sup>4</sup> has been analyzed by using a one-dimensional (1D) model<sup>6</sup> but it remains to be theoretically validated by using more realistic two-dimensional (2D) and three-dimensional (3D) models; (b) although polaronic<sup>4</sup> and bipolaronic<sup>9–11</sup> lattices have been proposed for doped PANI, solid and abundant experimental evidence strongly suggests that a combined model with the coexistence of polarons and bipolarons is very likely.<sup>12–20</sup> Depending on the preparation technique and composition of the sample, one of the two lattices can prevail over the other.<sup>21,22</sup> However, *ab initio* calculations<sup>6</sup> and Car–Parrinello molecular dynam-

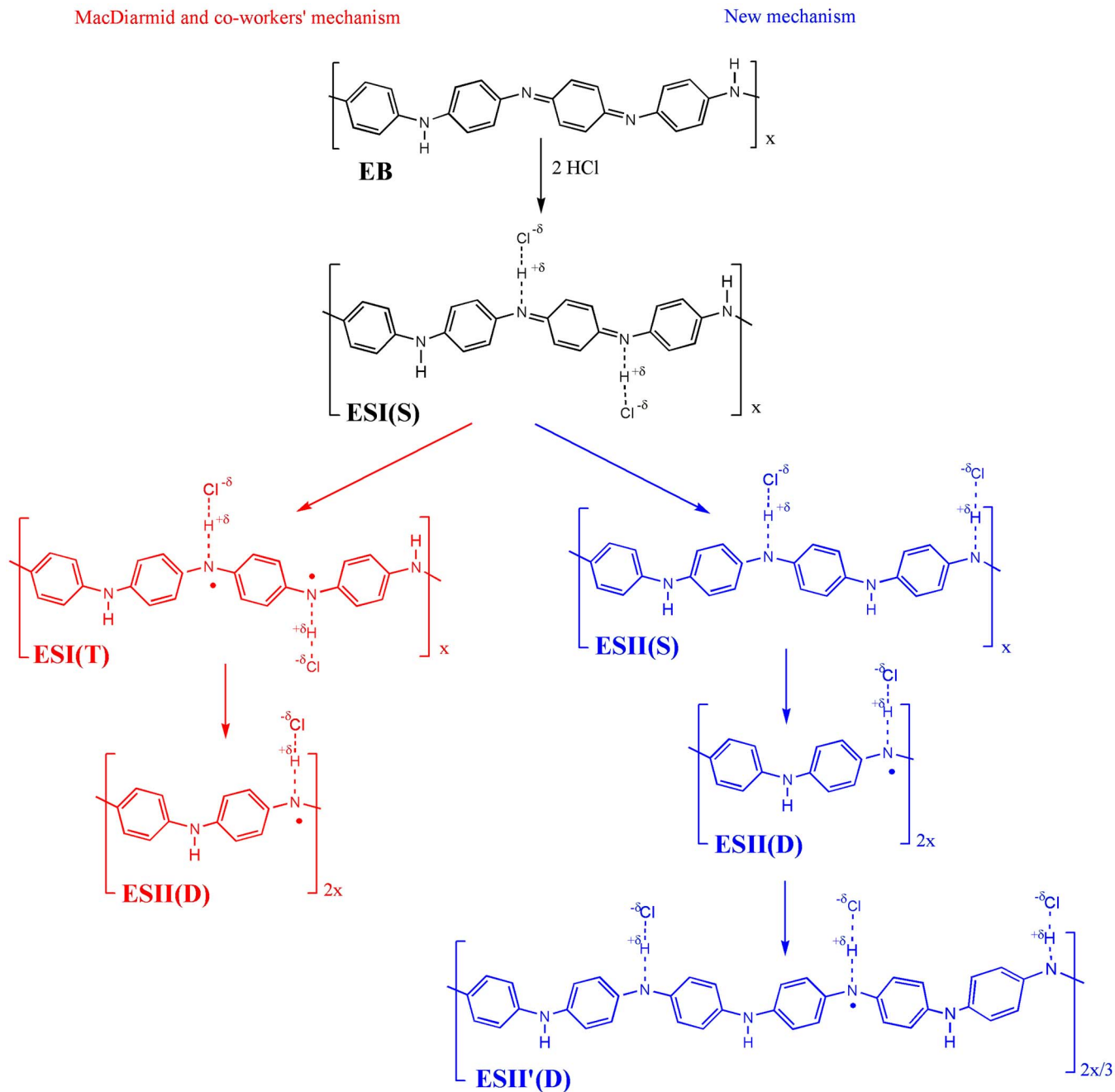
ics (CPMD) simulations<sup>7</sup> predict energy differences between polaron and bipolaron lattices to be greater than 11 kcal/mol. Consequently, only one of the two lattices should be present in any sample, (c) MacDiarmid and co-workers showed<sup>14,15</sup> that according to magnetic susceptibility measurements, there is a decrease in the number of spins at high level doping, and (d) they also reported that the initial protonation in the amorphous part of emeraldine base (the so-called EBII structure in Ref. 14) gives rise to a spinless charge state (bipolaron) until essentially maximum protonation is achieved in the amorphous region and the protonation begins to proceed in the crystalline regions with onset of Pauli susceptibility (polaron lattice).

The above points are addressed in the present article through the analysis of the results of an *ab initio* study on a 2D model of doped PANI. The structures involved in the mechanism proposed by Stafström *et al.*<sup>4</sup> (see Scheme 1), namely, emeraldine base [EB(S)], spinless charged bipolaron [ESI(S)], and charged radical open-shell polarons [ESI(T) and ESII(D)], together with two new bipolaronic [ESII(S)] and polaronic [ESII'(D)] structures, proposed here to play a mechanistic role (see below), have been studied. It will be shown that the structural, energetic, and spectroscopic theoretical predictions arising from the optimized geometries and density of state (DOS) curves are in good agreement with the available experimental data.

### METHODS

Density functional theory (DFT) with periodic boundary conditions were used to fully optimize the geometries. The selected DFT functional was the hybrid Perdew–Burke–Ernzerhof<sup>23</sup> (PBEh) in conjunction with Pople’s basis sets 6-31G(*d,p*).<sup>24</sup> This methodology has shown to provide a good description of 1D PANI. Indeed, our previous work<sup>6</sup> showed that the performance of hybrid functionals resulted much better than that corresponding to functionals derived within local density or generalized gradient approximations.<sup>25</sup> The energy was properly converged by employing no less than 400 *k*-points in every calculation. All calculations were carried out using GAUSSIAN 03 package

<sup>a)</sup> Author to whom correspondence should be addressed. Electronic mail: [jasg@uniovi.es](mailto:jasg@uniovi.es).



SCHEME 1. (Color online) Mechanisms for the formation of emeraldine salt (ES) from emeraldine base (EB) and HCl. The mechanism proposed by MacDiarmid and co-workers (red) and the new mechanism emerging from the present 2D calculations (blue) are depicted. Unit cells are shown for each structure. Multiplicity (*S*: Singlet, *D*: Doublet, and *T*: Triplet) is indicated in parentheses.

of programs,<sup>26</sup> which makes use of the fast multipole method for the evaluation of the long ranged electrostatic interactions, thus leading to a computationally very competitive linear scaling DFT implementation.

## GEOMETRIES AND ENERGETICS

The 2D structures considered in the present work are shown in Fig. 1 and some representative geometrical parameters are collected in Table I. According to Stafström *et al.*,<sup>4</sup> protonation of emeraldine base EB(*S*) leads to a spinless charged (bipolaronic) structure ESI(*S*), which rearranges to a charged radical open-shell (polaronic) triplet structure

ESI(*T*). Finally, this latter structure splits into two units (subscript  $2x$  in Scheme 1) of the polaronic structure ESII(*D*).

Alternatively, the chlorine atoms in ESI structures can shift apart, giving rise to the singlet structure ESII(*S*). We have also considered the ESII'(*D*) structure in which three consecutive ESII(*D*) polaronic defects in the lattice couple two spins leading to the six-rings single-radical (polaronic) unit cell shown in Scheme 1.

Examination of Table I shows the 2D geometrical parameters theoretically predicted for EB and the different forms of ES to agree reasonably well, in general, with the available experimental data.

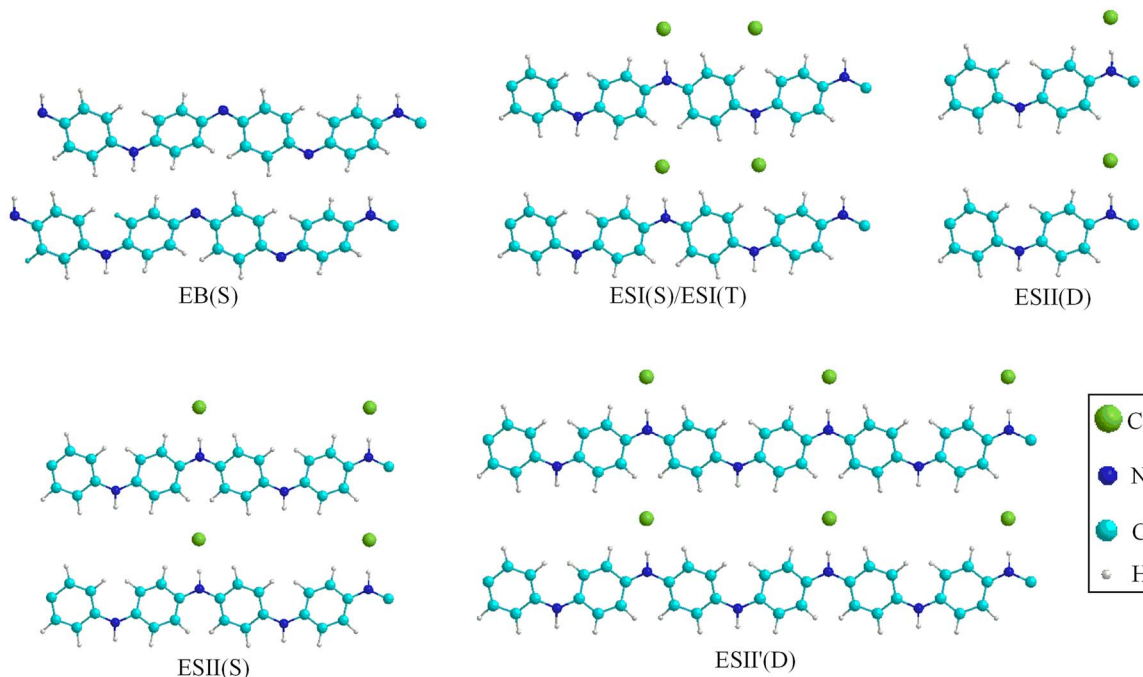


FIG. 1. (Color online) 2D structures considered in the present work. Multiplicity (*S*: Singlet, *D*: Doublet, and *T*: Triplet) is indicated in parentheses. Scheme 1 shows some electronic details of the different structures.

Table II collects the electronic energy of the structures under study. A recent 3D CPMD study<sup>7</sup> on PANI has shown that the interchain  $\pi$ - $\pi$  (up-down) interactions are much less important than side interactions between chains. Indeed, the rupture of the  $\pi$ - $\pi$  interactions, passing from a *Pc2a* to a *P2<sub>1</sub>22<sub>1</sub>* orthorhombic polaronic structure costs only about 0.1 eV ( $\sim 2$  kcal/mol) according to CPMD calculations.<sup>7</sup> Bearing in mind that consideration of a 3D model through an *ab initio* conventional formulation of electronic structure calculations would become impractical from the computational viewpoint, we focused on a 2D model including the relevant interchain side interactions (see Fig. 1).

The polaron lattice ESII(*D*) allowed Stafström *et al.* to explain, through semiempirical approaches,<sup>4</sup> most of the electric, magnetic, optical, and structural properties experi-

mentally measured for doped PANI.<sup>5</sup> While *ab initio* calculations on a 1D model suggested that the bipolaronic structure ESI(*S*) resulted lower in energy,<sup>6</sup> CPMD 3D calculations led to the conclusion that ESII(*D*) is more stable.<sup>7</sup> Consideration of the present 2D model demonstrates that the interchain side interactions greatly contribute to stabilize the polaronic structure ESII(*D*) that lies only 2.5 kcal/mol above ESI(*S*). This is a very important result because the two previous theoretical works<sup>6,7</sup> predicted huge energy differences ( $> 11$  kcal/mol) between polaron and bipolaron structures, thus making it impossible to rationalize the experimentally observed equilibrium between these two lattices.<sup>12–20</sup> Furthermore, exploiting our computer capabilities until the very limit (837 basis functions), we computed the stability of a

TABLE I. Some selected geometrical parameters estimated at the PBEh/6-31G(*d,g*) level.  $\alpha$ ,  $b$ , and  $c$  are the usual cell parameters and  $\phi_X$  ( $X=A, B, C, D, E, F$ ) represents the dihedral angle between the virtual plane defined by the nearly coplanar nitrogen atoms and the  $C_6$  rings (from left to right in Fig. 1) in the different structures. The values in parentheses correspond to the 1D estimates. The experimental values available (Expt.) are also collected. Distances are given in Å and angles in deg.

	EB	Expt. EB <sup>a</sup>	ESI	ESII( <i>S</i> )	ESII( <i>D</i> )	ESII'( <i>D</i> )	Expt. ES <sup>a</sup>
$\phi_A$	20 (21)		30 (27)	20	19 (22)	19	
$\phi_B$	40 (39)		21 (26)	10	18 (21)	14	
$\phi_C$	12 (10)	30	7 (10)	22		22	0–15
$\phi_D$	40 (37)		21 (25)	12		17	
$\phi_E$						19	
$\phi_F$						15	
$b$	6.023	5.65–5.75	8.020	8.051	8.026	8.034	7.9–8.6
$c$	20.128 <sup>b</sup>	10.05–10.40	20.477 <sup>b</sup>	20.657 <sup>b</sup>	10.256	30.805 <sup>c</sup>	10.4
$\alpha$	105.4	90	89.4	90.0	90.0	90.0	90

<sup>a</sup>Reference 33.

<sup>b</sup>The actual periodicity is  $2c$  according to Fig. 1 (see Ref. 33).

<sup>c</sup>The actual periodicity is  $3c$  according to Fig. 1 (see Ref. 33).



TABLE II. Absolute ( $E$ ; a.u.) and relative ( $\Delta E$ ; kcal/mol) electronic energies computed for the PANI structures under study.

Structure	$E$	$\Delta E^a$
EB	-11.43.088 758	
HCl	-460.631 044 0	
ESI( $S$ )	-2064.420 619	-43.8
ESI( $T$ ) <sup>b</sup>	...	...
ESII( $S$ )	-2064.416 213	-41.0
ESII( $D$ )	-1032.207 520	-40.3
ESII'( $D$ )	-3096.631 569	-44.1

<sup>a</sup> $\Delta E = nE(\text{ESX}) - E(\text{EB}) - 2E(\text{HCl})$ , where  $\text{ESX} = \text{ESI}(S)$ ,  $\text{ESI}(T)$ ,  $\text{ESII}(S)$ ,  $\text{ESII}(D)$ ,  $\text{ESII}'(D)$ , and  $n$  is the factor multiplying subscript  $x$  in the structures collected in Scheme 1.

<sup>b</sup>This structure is not present on the 2D potential energy surface.

new polaron lattice,  $\text{ESII}'(D)$ , not considered by Stafström *et al.*, formally arising from the intrachain interaction between a polaron and a bipolaron in  $\text{ESII}$ . In this new structure  $\text{ESII}'(D)$ , a trication single-radical lattice<sup>27</sup> is formed, thus reducing the ratio between the number of spins and the number of dopant charges. Formally,  $\text{ESII}'(D)$  can be thought to be formed as a consequence of the spin coupling between two consecutive  $\text{ESII}(D)$  polaron defects in a virtual  $\text{ESII}(D)$ - $\text{ESII}(D)$ - $\text{ESII}(D)$  unit cell. According to our calculations,  $\text{ESII}'(D)$  becomes slightly more stable (by 0.3 kcal/mol) than bipolaron lattice  $\text{ESI}(S)$ . Therefore, the new polaron structure allows us to explain the appearance of electron spin resonance (ESR) signal and the decrease in the number of spins at high doping level, both experimentally observed in emeraldine salt.<sup>28</sup>

Another interesting feature we detected is the strong destabilization, affecting the  $\text{ESI}(T)$  polaron structure when passing from 1D (Ref. 6) to the present 2D model. Indeed, no such a structure could be characterized as a minimum on the 2D potential energy hypersurface. Instead, we located a new bipolaron structure,  $\text{ESII}(S)$ , which is only 2.8 kcal/mol less stable than  $\text{ESI}(S)$ . This result suggests a new mechanism for the formation of doped emeraldine, which is compatible with all the experimental facts (see Mechanism section below).

## BAND STRUCTURE

Figure 2 shows the band structure and the corresponding DOSs for the five structures in Fig. 1 located on the 2D potential energy hypersurface. In the following discussion, the theoretical absorption bands were estimated from the direct gaps between the occupied and virtual bands.

In the case of EB phase, the experimental photoemission spectrum shows two transitions:<sup>29,30</sup> (a) A strong absorption centered at 2 eV and (b) an absorption band (the  $\pi \rightarrow \pi^*$  band gap) at 3.6 (solution) or 3.8 eV (film). Our PBEh calculations (see Fig. 2) predict a first transition from the highest occupied crystal orbital (HOCO) to the lowest unoccupied crystal orbital (LUCO) at 2.1–2.6 eV, and a second broad absorption starting at 4.3 eV. Therefore, the agreement between the experimental observation and the theoretical predictions is reasonably good.

For the conducting (salt) form,<sup>4</sup> there are two strong optical peaks at 2.8 and 4.1 eV, and a broad absorption at 1.5 eV. Similarly to what we found in our previous 1D study on PANI,<sup>6</sup> the 2D PBEh/6-31G( $d,p$ ) calculations predict transitions for the four structures of emeraldine salt considered in the present work, namely,  $\text{ESI}(S)$ ,  $\text{ESII}(S)$ ,  $\text{ESII}(D)$ , and  $\text{ESII}'(D)$  (see Scheme 1), which are fully compatible with the optical absorption spectra of protonated PANI. Indeed, Fig. 2 shows that the band structures predict HOCO  $\rightarrow$  LUCO transitions at 1.4–2.2 eV [ $\text{ESI}(S)$ ], 0.3–1.9 eV [ $\text{ESII}(S)$ ], and 1.2–2.0 eV [ $\text{ESII}(D)$ ] as well as broad  $\pi \rightarrow \pi^*$  bands starting at 4.5 eV [ $\text{ESI}(S)$ ] and 4.0 eV [ $\text{ESII}(S)$ ,  $\text{ESII}(D)$ ]. In the case of  $\text{ESII}'(D)$ , its band structure predicts HOCO  $\rightarrow$  LUCO, LUCO+1, and LUCO+2 transitions from 1.3 to 1.9 eV and a  $\pi \rightarrow \pi^*$  band starting at 4.2 eV. For all the emeraldine salt model structures, 2D calculations predict a band absorption at 2.8 eV, involving the LUCO and some occupied crystal orbitals close to the HOCO-1.

## MECHANISM

The results presented and analyzed in the previous sections suggest some modifications of the original mechanism proposed by Stafström *et al.* 20 years ago,<sup>4</sup> based on calculations carried out by using the one-electron valence effective Hamiltonian formalism, to explain the transformation between emeraldine base and emeraldine salt. The new mechanism is sketched in Scheme 1.

In agreement with the proposal of Stafström *et al.*, in a first step, emeraldine base EB gives rise to a bipolaronic structure  $\text{ESI}(S)$  as a consequence of the HCl doping. However, unlike the original proposal, the new mechanism does not need to resort to a quinoid-to-benzenoid transformation through an internal redox reaction leading to the charged radical open-shell structure  $\text{ESI}(T)$ . As mentioned in the Geometries and Energetics section, this latter lattice was characterized in our previous 1D calculations but it is not present on the 2D potential energy hypersurface. We propose, as an alternative, a quinoid-to-benzenoid transformation provoked by a shifting of the counterions (chlorine atoms; see Fig. 1). The energetic cost to promote the  $\text{ESI}(S) \rightarrow \text{ESII}(S)$  transformation is only 2.8 kcal/mol according to Table II.

An almost energetically inexpensive (0.8 kcal/mol) electronic rearrangement in  $\text{ESII}(S)$  leads to the  $\text{ESII}(D)$  structure, postulated by Stafström *et al.* to be the polaronic lattice responsible for the very special properties exhibited by emeraldine salt. Finally, intrachain interactions between two consecutive unit cells in the  $\text{ESII}(D)$  lattice leads to the more stable trication single-radical (polaronic) lattice  $\text{ESII}'(D)$ , which, according to our 2D calculations, is the most stable phase of emeraldine salt (see Table II).

Thus,  $\text{ESII}'(D)$  represents a very suitable model for emeraldine salt. On the one hand, its structural parameters (see Table I) and band structure (see Fig. 2) are fully consistent with x-rays information and optical absorption data available, as noted in the preceding sections. On the other hand, the polaronic nature of this lattice does support the appearance of ESR signal. Furthermore, the decrease in the

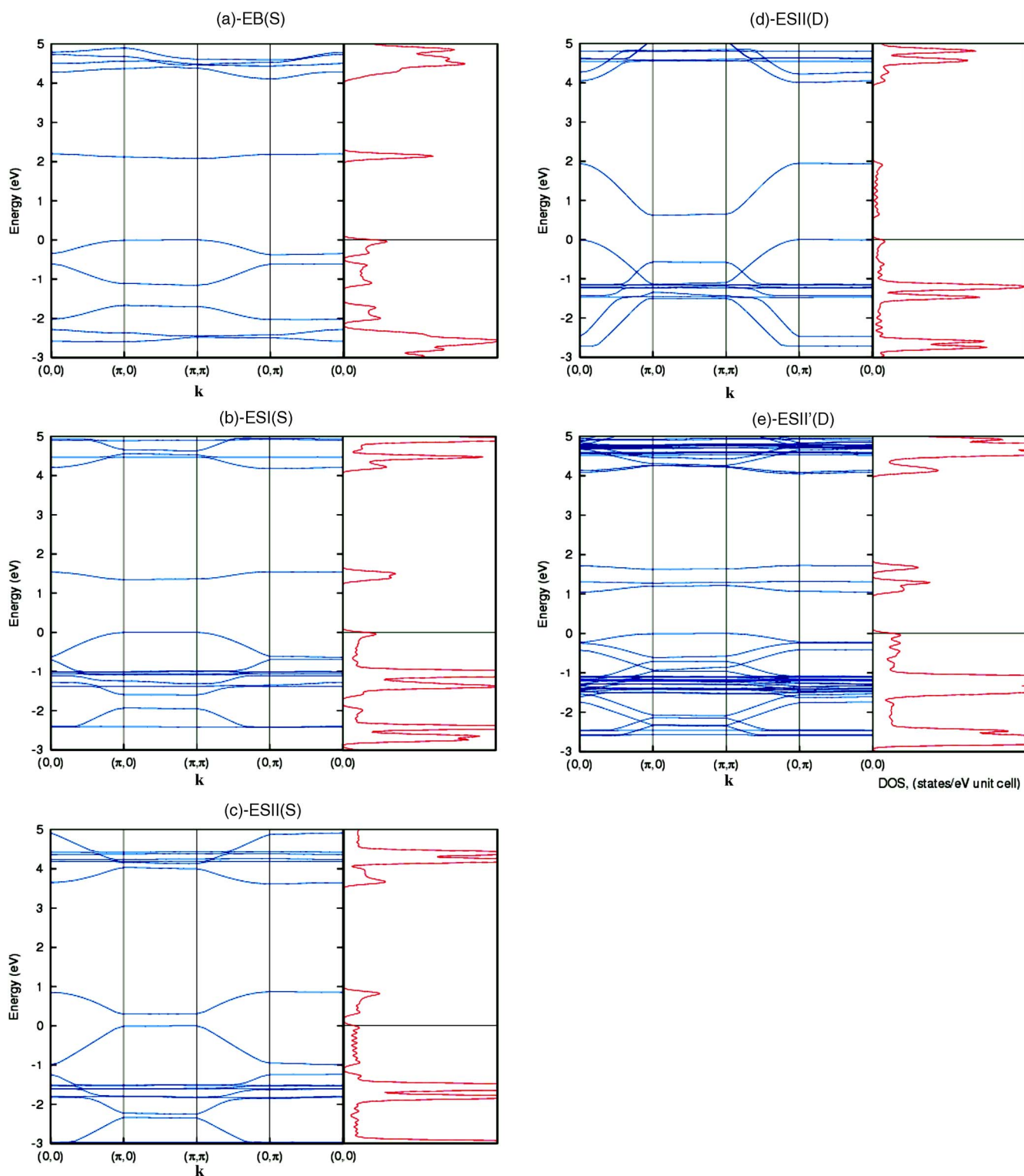


FIG. 2. (Color online) Band structure and density of states for the 2D structures considered in the present work as computed at the PBEh/6-31G(*d,p*) level.

number of spins detected at high doping levels in magnetic susceptibility experiments<sup>28</sup> can be ascribed to the ESII(*D*)-ESII(*D*)-ESII(*D*) (trication triple-radical)  $\rightarrow$  ESII'(*D*) (trication single-radical)<sup>27</sup> transformation.

Another important point is the small energy difference between bipolaron ESI(*S*) and polaron ESII'(*D*) lattices predicted by our 2D PBEh/6-31G(*d,p*) calculations (0.3 kcal/mol, favoring the latter). This fact leads to the con-

clusion that the real picture of doped PANI emerging from the present study is a ESI(*S*) [bipolaron]  $\rightleftharpoons$  ESII'(*D*) [polaron] thermodynamic equilibrium shifted toward the polaronic lattice, in full agreement with experimental evidence.<sup>12-20</sup> Neither CPMD simulations<sup>7</sup> nor *ab initio* 1D calculations<sup>6</sup> were able to predict the coexistence of both lattices. Indeed, both methodologies predict a huge energy difference ( $>11$  kcal/mol) between them.

It is well known that when trying to get a deeper insight into the nature of the metallic state of conducting polymers, a number of issues arise. The first one refers to the dimensionality (1D versus 3D) of the metallic states. Conduction and charge transport mechanisms in doped PANI have historically been explained by means of 1D (disordered-amorphous)<sup>11,31</sup> and 3D (ordered-crystalline)<sup>32</sup> models. MacDiarmid and co-workers have stressed the experimental evidence that while metallic Pauli susceptibility is detected in the ordered regions, predominantly spinless bipolarons are present in the disordered doped PANI.<sup>14,15,18,33</sup>

A second factor that plays a relevant role in charge transport is the interchain interaction. While the existence of a 3D homogeneous disorder, arising as a consequence of substituent interactions between polymer chains, has been suggested,<sup>34</sup> MacDiarmid and co-workers proposed an inhomogeneous disorder model in which ordered (crystalline) regions, described by 3D metallic states, are connected through amorphous regions of polymer chains where 1D disorder-induced localization is dominant.<sup>18</sup>

Another issue focuses on the way charge transport takes place. While a quasi-1D model emphasizes nearest-neighbor interchain hopping in disordered regions, the so-called granular metallic model,<sup>35</sup> which is based on the original proposal for a granular metal of Sheng *et al.*,<sup>36</sup> uses charge tunneling between metallic islands.

Joo *et al.*<sup>18</sup> proposed a model (inhomogeneous disorder model) for doped PANI in which 3D metallic bundles, corresponding to the more ordered (crystalline) regions, are coupled in the 3D network by single chains (1D) in the less ordered (amorphous) regions of the material.<sup>18,37</sup> They showed that that model allowed for the rationalization of a number of experimental properties measured for different samples of doped PANI. Our calculations provide a theoretical support for that model. Indeed, the 1D model employed in our earlier study on doped PANI (Ref. 6) suggested that a spinless bipolaron lattice is the most stable structure. Inclusion of side interactions between chains, present in 2D and 3D models, leads to the above-mentioned conclusion that the equilibrium between bipolaron and polaron lattices, slightly shifted toward the latter form, is established.

It should be finally stressed that the computed greater stability of the polaronic lattice ESII'(D) proposed in the new mechanism makes the formation of the 3D metallic islands postulated in inhomogeneous disorder model of Joo *et al.* possible.<sup>18</sup>

We also notice that our calculations show that the interchain side interactions contribute to the generation of more planar chain conformations for emeraldine salt (2D torsion angles between phenyl ring and the plane of the backbone are somewhat smaller than the corresponding 1D ones; see Table I). Lee *et al.*<sup>38</sup> have recently emphasized that such a situation allows for an improved carrier transport in doped PANI.

## CONCLUSION

The results reported in the present work represent a step forward in the understanding of the mechanism of formation

of conducting polymers. The analysis of the structures involved and their relative energies helped us to rationalize the mechanism of formation of emeraldine salt from HCl doping of emeraldine base. The results of some crucial experimental results on doped PANI, namely, the existence of polaron-bipolaron equilibrium, its magnetic behavior, and the "metallic island" model for conduction proposed for emeraldine salt, have been rationalized in terms of a trication single-radical (polaron) lattice, which, according to periodic boundary condition PBEh/6-31G(*d,p*) calculations, is the most stable phase of doped PANI. The structural parameters and the optical transitions predicted for that lattice are in good agreement with x-ray information and optical absorption data available for emeraldine salt.

## ACKNOWLEDGMENTS

The authors thank partial financial support by MEC (Madrid, Spain) under Project No. CTQ2007-67234-C02-01/BQU.

- <sup>1</sup>H. Shirakawa, E. J. Lewis, A. G. MacDiarmid, C. K. Chiang, and A. J. Heeger, *J. Chem. Soc., Chem. Commun.* **1977**, 578.
- <sup>2</sup>C. K. Chiang, C. R. Fincher, Jr., Y. W. Park, A. J. Heeger, H. Shirakawa, E. J. Louis, S. C. Gau, and A. G. MacDiarmid, *Phys. Rev. Lett.* **39**, 1098 (1977).
- <sup>3</sup>A. G. MacDiarmid, *Synth. Met.* **125**, 11 (2002).
- <sup>4</sup>S. Stafström, J. L. Bredas, A. J. Epstein, H. S. Woo, D. B. Tanner, W. S. Huang, and A. G. MacDiarmid, *Phys. Rev. Lett.* **59**, 1464 (1987).
- <sup>5</sup>A. J. Heeger, *J. Phys. Chem. B* **105**, 8475 (2001).
- <sup>6</sup>A. Varela-Álvarez, J. A. Sordo, and G. E. Scuseria, *J. Am. Chem. Soc.* **127**, 11318 (2005).
- <sup>7</sup>C. Cavazzoni, R. Colle, R. Farchioni, and G. Grosso, *Phys. Rev. B* **74**, 033103 (2006).
- <sup>8</sup>R. Colle, P. Parruccini, A. Benassi, and C. Cavazzoni, *J. Phys. Chem. B* **111**, 2800 (2007).
- <sup>9</sup>D. S. Galvao, D. A. dos Santos, B. Laks, C. P. de Melo, and M. J. Caldas, *Phys. Rev. Lett.* **63**, 786 (1989).
- <sup>10</sup>H.-L. Wu and P. Phillips, *Phys. Rev. Lett.* **66**, 1366 (1991).
- <sup>11</sup>F. C. Lavarada, M. C. dos Santos, D. S. Galvao, and B. Laks, *Phys. Rev. Lett.* **73**, 1267 (1994).
- <sup>12</sup>E. M. Genies and M. Lapkowski, *J. Electroanal. Chem. Interfacial Electrochem.* **220**, 67 (1987).
- <sup>13</sup>E. M. Genies and M. Lapkowski, *J. Electroanal. Chem. Interfacial Electrochem.* **236**, 199 (1987).
- <sup>14</sup>M. E. Jozefowicz, R. Laversanne, H. H. S. Javadi, A. J. Epstein, J. P. Pouget, X. Tang, and A. G. MacDiarmid, *Phys. Rev. B* **39**, 12958 (1989).
- <sup>15</sup>A. G. MacDiarmid and A. J. Epstein, *Faraday Discuss. Chem. Soc.* **88**, 317 (1989).
- <sup>16</sup>M. Lapkowski and E. M. Genies, *J. Electroanal. Chem. Interfacial Electrochem.* **279**, 157 (1990).
- <sup>17</sup>S. M. Yang and C. P. Li, *Synth. Met.* **55**, 636 (1993).
- <sup>18</sup>J. Joo, S. M. Long, J. P. Pouget, E. J. Oh, A. G. MacDiarmid, and A. J. Epstein, *Phys. Rev. B* **57**, 9567 (1998).
- <sup>19</sup>V. Luthra, R. Singh, S. K. Gupta, and A. Mansingh, *Curr. Appl. Phys.* **3**, 219 (2003).
- <sup>20</sup>A. Petr, A. Neudeck, and L. Dunsch, *Chem. Phys. Lett.* **401**, 130 (2005).
- <sup>21</sup>Y. Long, Z. Chen, J. Shen, Z. Zhang, L. Zhang, H. Xiao, M. Wan, and J. L. Duvail, *J. Phys. Chem. B* **110**, 23228 (2006).
- <sup>22</sup>S. Bhadra, N. K. Singha, and D. Khastgir, *Synth. Met.* **156**, 1148 (2006).
- <sup>23</sup>J. P. Perdew, K. Burke, and M. Ernzerhof, *J. Chem. Phys.* **105**, 9982 (1996).
- <sup>24</sup>W. J. Hehre, L. Radom, P. v. R. Schleyer, and J. A. Pople, *Ab initio Molecular Orbital Theory* (Wiley, New York, 1986).
- <sup>25</sup>C. J. Cramer, *Essentials of Computational Chemistry. Theories and Models* (Wiley, Baffins Lane, 2002).
- <sup>26</sup>M. J. Frisch, C. W. Trucks, H. B. Schlegel *et al.*, GAUSSIAN03, C.01, Gaussian, Inc., Wallingford, CT, 2004.
- <sup>27</sup>Y. Furukawa, *J. Phys. Chem.* **100**, 15644 (1996).

- <sup>28</sup> J. M. Ginder, A. F. Richter, A. G. MacDiarmid, and A. J. Epstein, *Solid State Commun.* **63**, 97 (1987).
- <sup>29</sup> R. P. McCall, J. M. Ginder, J. M. Leng, H. J. Ye, S. K. Manohar, J. G. Masters, G. E. Asturias, and A. G. MacDiarmid, *Phys. Rev. B* **41**, 5202 (1990).
- <sup>30</sup> J. M. Leng, R. P. McCall, K. R. Cromack, Y. Sun, S. K. Manohar, A. G. MacDiarmid, and A. J. Epstein, *Phys. Rev. B* **48**, 15719 (1993).
- <sup>31</sup> P. Phillips and H.-L. Wu, *Science* **252**, 1805 (1991).
- <sup>32</sup> Z. H. Wang, C. Li, E. M. Scherr, A. G. MacDiarmid, and A. J. Epstein, *Phys. Rev. Lett.* **66**, 1745 (1991).
- <sup>33</sup> J. P. Pouget, M. E. Józefowicz, A. J. Epstein, X. Tang, and A. G. MacDiarmid, *Macromolecules* **24**, 779 (1991).
- <sup>34</sup> N. J. Pinto, P. K. Kahol, B. J. McCormick, N. S. Dalal, and H. Wan, *Phys. Rev. B* **49**, 13983 (1994).
- <sup>35</sup> Q. Li, L. Cruz, and P. Phillips, *Phys. Rev. B* **47**, 1840 (1993).
- <sup>36</sup> P. Sheng, B. Abeles, and Y. Arie, *Phys. Rev. Lett.* **31**, 44 (1973).
- <sup>37</sup> J. Joo, V. N. Progodin, Y. G. Min, A. G. MacDiarmid, and A. J. Epstein, *Phys. Rev. B* **50**, 12226 (1994).
- <sup>38</sup> K. Lee, S. Cho, S. H. Park, A. J. Heeger, C.-W. Lee, and S.-H. Lee, *Nature (London)* **441**, 65 (2006).